35th Annual International Conference of the IEEE EMBS
Osaka, Japan, 3 - 7 July, 2013

Fully Automated Segmentation of Corpus Callosum in Midsagittal Brain MRIs

Yue Li, Mrinal Mandal, *Senior Member IEEE*, and S. Nizam Ahmed

***Abstract*— In the diagnosis of various brain disorders by analyzing the brain magnetic resonance images (MRI), the segmentation of corpus callosum (CC) is a crucial step. In this paper, we propose a fully automated technique for CC segmentation in the T1-weighted midsagittal brain MRIs. An adaptive mean shift clustering technique is first used to cluster homogenous regions in the image. In order to distinguish the CC from other brain tissues, area analysis, template matching, in conjunction with the shape and location analysis are proposed to identify the CC area. The boundary of detected CC area is then used as the initial contour in the Geometric Active Contour (GAC) model, and evolved to get the final segmentation result. Experimental results demonstrate that the proposed technique overcomes the problem of manual initialization in existing GAC technique, and provides a reliable segmentation performance.**

I. Introduction

The corpus callosum (CC) is the largest white-matter structure in human brain. It connects the left and right cerebral hemispheres, and works for interhemispheric communication. Several neuroimaging studies have revealed that the structural changes of CC occur in a variety of neurological diseases, such as epilepsy [1] and autism [2]. If the CC area can be segmented correctly, anatomical and structural features, such as size and shape, can be used to determine the condition of neurological diseases.

The in-vivo Magnetic Resonance Imaging (MRI) is regarded as the best approach for obtaining the structural information of CC, such as cross-sectional area and shape [3]. Typically, in the T1-weighted midsagittal brain MRI, CC has the appearance of broad arched band. An example of the T1-weighted midsagittal brain MRI slice is illustrated in Fig. 1(a). Note that the yellow contour indicates the CC structure. It is observed that the CC structure is horizontal oriented, and located near the centre of the brain. One close-up example of CC is shown in Fig. 1(b), where the CC area is highlighted by yellow contour. CC area presents high intensity, and appears as a narrow and long shape. The location and shape of CC are important features to distinguish CC from other brain tissues.

Segmentation of CC from brain MRIs is a challenging and critical task in medical image analysis. Several works have been conducted on the segmentation of CC in brain MRIs. Ginneken et al. [4] proposed a technique for CC extraction in brain MRIs using the learned CC shape model. El-Baz et al. [5] proposed an improved segmentation technique using the learned CC shape model and the visual appearance model. However, the performances of both techniques are sensitive to training images. Jacob et al. [6] proposed an Active Contour Model (ACM) based technique for CC segmentation, and the contour evolves by minimizing the energy functionals related to the current contour. Sandhu et al. [7] proposed a Geometric Active Contour (GAC) based segmentation technique, where the region information is incorporated. Although these ACM based techniques have been reported to provide good performance, there are still some limitations: (i) an initial contour is required from user inputs; (ii) ACM may fail if the initial contour is far from the boundary of interested object.

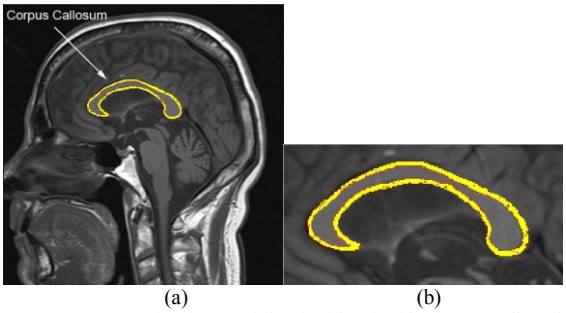

(a) (b)

Figure 1. (a) An example of T1-weighted midsagittal brain MRI slice, the CC area is highlighted by yellow contour. (b) A close up example of the CC.

To address the limitations of ACM based segmentation technique, we propose a hybrid technique for automated CC segmentation, which outperforms the existing techniques. In the proposed technique, using the adaptive mean shift clustering technique, the image is first clustered into various homogeneous areas, representing various brain tissues. The CC area is then detected based on area analysis, template matching, in conjunction with shape and location analysis. The boundary of obtained CC area is extracted and evolved under the mechanism of GAC model, for final segmentation of CC structure. The major contribution of the proposed technique is to provide an accurate initialization of the CC region, which results in better performance in terms of the segmentation accuracy.

The rest of the paper is organized as follows: Section 2 introduces details of the proposed technique. Section 3 shows the experimental results tested on real brain MRI data, followed by the conclusion in Section 4.

II. The Proposed Technique

The schematic of the proposed technique is shown in Fig. 2. It is observed that the technique contains three modules: Adaptive Mean Shift Clustering, Automated Initialization of CC Contour, Geometric Active Contour based Segmentation. Details of each module are presented in the following.

Y. Li and M. Mandal are with the Department of Electrical and Computer Engineering, University of Alberta, Edmonton, AB, T6G 2V4, Canada (corresponding author to provide phone: +1 780-492-0294; fax: +1 780-492-1811; email: mmandal@ualberta.ca).

S. N. Ahmed is with the Department of Medicine, University of Alberta, Edmonton, AB, T6G 2V4, Canada (e-mail: snahmed@ualberta.ca).

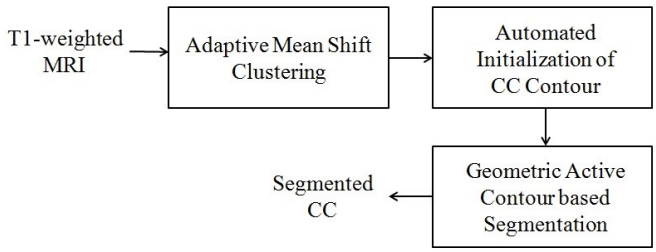

Figure 2. Schematic of the proposed technique

A. Adaptive Mean Shift Clustering

In most MRIs, CC area is an area with homogeneous intensity. In this work, we use an adaptive mean shift (AMS) technique [8] to cluster homogenous areas. The AMS is a useful tool for finding modes (stationary points of the density of image intensity) of an image. The steps for image clustering using adaptive mean shift technique [8] are as follows:

1) Consider an image with N pixels, and consider the gray scale intensity g as a 1-D feature vector for N pixels. For each pixel i in the image, let its feature vector be denoted by V_i. Calculate the Euclidean distance between V_i and its neighbors, and sort these neighbors of V_i by order of increasing distance to V_i. Let $V_{i,k}$ denote the k^{th}-nearest neighbor of V_i. We set k=50 experimentally, as k increases, the number of clusters decreases. The adaptive bandwidth h_i is calculated as follows,

$$h_i = \left\| V_i - V_{i,k} \right\|_2 . \tag{1}$$

2) For each feature vector V_i, a symmetric window S_h with bandwidth h_i is generated. Let the number of points included in S_h be J_i (including V_i).

3) For each feature vector V_i within the window S_h, calculate the weighted mean shift vector $M_h(V_i)$ using the equation as follows,

$$M_h(V_i) = \frac{\sum_{j=1}^{J_i} \frac{1}{h_i^{d+2}} (V_j - V_i) \cdot K\left(\frac{V_j - V_i}{h_i} \right)}{\sum_{j=1}^{J_i} \frac{1}{h_i^{d+2}} K\left(\frac{V_j - V_i}{h_i} \right)}, \tag{2}$$

where V_j is the j^{th} feature vector within window S_h, and d is the dimension of feature space, in our case, d=1. $K(x)$ is the kernel function and is calculated as follows,

$$K(\mathbf{x}) = \begin{cases} c\left(1 - \|\mathbf{x}\|_2^2\right) & \|\mathbf{x}\|_2 \le 1 \\ 0 & \text{otherwise} \end{cases}, \tag{3}$$

where c is a normalization constant that makes the integral of $K(x)$ equals to one.

4) Shift the center of window V_i by $M_h(V_i)$, and repeat till the norm of $M_h(V_i)$ is less than 1, and store the convergence points as modes, which are centers of different homogeneous regions in the image.

An illustrative example is shown in Fig. 3. A T1-weighted brain MRI is shown in Fig. 3(a), and the resulting cluster map generated by the AMS is shown in Fig. 3(b). Note that the vicinity pixels that have similar intensity values are clustered.

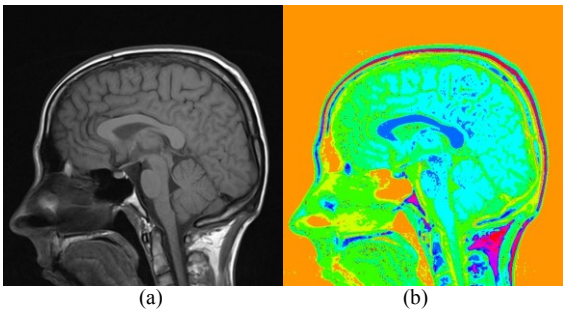

(a) (b)

Figure 3. (a) An input midsagittal T1-weighted brain MRI. (b) Resulting cluster map generated by AMS

B. Automated Initialization of CC Contour

In the subsequent processing, the Geometric Active Contour (GAC) Model [7] is adopted to segment the CC, and a specific initialization of contour is required before applying the GAC technique. In order to find the initial area of CC automatically, we propose a hybrid initialization technique which is presented below.

1) Area Analysis: In order to automatically identify a CC cluster from all clusters generated by the AMS technique, the area analysis criterion is applied. Based on the prior knowledge, the CC is within a predefined threshold range $[T_{al}, T_{ah}]$. We set $T_{al}=N \times 1.5\%$ and $T_{ah}=N \times 9\%$ experimentally, where N is the total number of pixels in the brain MRI. The fractions 1.5% and 9% are determined based on the domain prior and experimental results. By applying the area criterion to the pre-clustered regions, we obtain a binary image with a few candidate regions. Denote this binary image as I_B.

2) Template Matching: As shown in Fig. 3 (a), besides the true CC, there exist a few unrelated regions. Therefore, in this step, the template matching (TM) technique is applied to detect the true CC area. This step has several sub steps and discussed as follows.

At first, we generate a set of template images. The template images are generated based on a CC structure from a healthy person provided by a radiologist. Based on the knowledge of CC, we could build template images for matching with various sizes, shear and orientations by changing the scales, rotation angles, and shear transform parameter. In this work, the horizontal scale factor S_x and vertical scale factor S_y are changed in the range of [0.8, 1] with a step of 0.1. The clockwise rotation angle θ includes -15°, 0°, 15°, 30°, and the shear transform parameter [Sh_x, Sh_y] are both within [0, 0.15] with a step of 0.05. The scale [S_x, S_y], rotation angle θ and shear transform parameter [Sh_x, Sh_y] are incorporated using the following equations,

$$x_s = S_x x, \quad y_s = S_y y , \tag{4}$$

$$x_r = x\cos\theta + y\sin\theta, \quad y_r = y\cos\theta - x\sin\theta , \tag{5}$$

$$x_{sh} = x + sh_y \cdot y, \quad y_{sh} = sh_x \cdot x + y . \tag{6}$$

In total, the template image dataset contains 48 templates. Examples of CC templates are shown in Fig. 4.

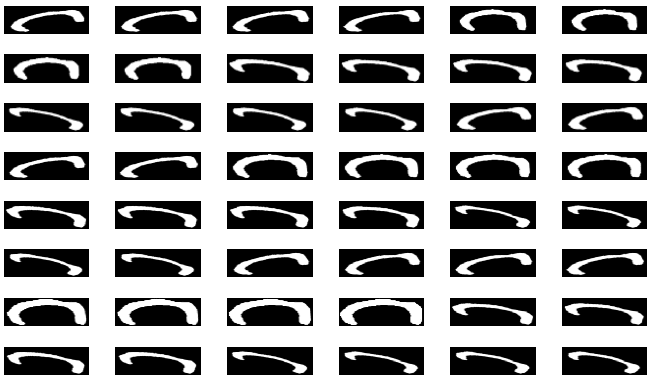

Figure 4. An example of CC templates, S_x within [0.8, 1], S_y within [0.8, 1], θ = -15°, 0°, 15°, 30°, shear parameter within [0, 0.15]

Given the dataset of CC templates, each template is translated to every possible location in the binary image I_B. The similarity between a template t and a sub-image f is measured by calculating the value of normalized cross correlation (NCC) [9], which is defined as,

$$NCC(f,t) = \frac{\sum_{x,y}[f(x,y) - \overline{f}_{u,v}][t(x-u,y-v) - \overline{t}]}{\{\sum_{x,y}[f(x,y) - \overline{f}_{u,v}]^2[t(x-u,y-v) - \overline{t}]^2\}}, \quad (7)$$

where *f(x,y), (u,v)* and $\overline{f}_{u,v}$ are the pixel, centre and mean of the sub-image respectively, whereas *t(x-u,y-v)* and $\overline{t}$ are the pixel and mean of the template respectively. The value of NCC is between 0 and 1, and higher value indicates higher similarity. To identify a true CC area, we use a similarity criterion. The sub-image *f* satisfying the following condition

$$NCC(f,t) > T_{NCC}, \quad (8)$$

will be considered as a true CC area. In this work, the predefined threshold T_{NCC} is set to 0.7 empirically.

3) Shape and Location Analysis: Based on observation, CC structure is generally longer than its width, and located near the center of the image. The shape feature can be represented by the ratio of the major axis length (l_1) and minor axis length (l_2) of the best fit ellipse [10]. In order to extract the location feature, first, we calculate the distance l_d between the image centre and the centre of detected CC area, and then we calculate the ratio of l_d to the image height (l_h). This ratio is considered as the location feature of CC.

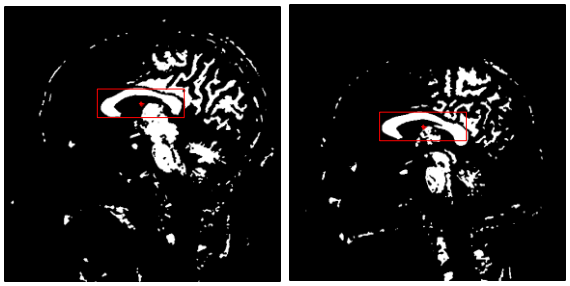

(a) (b)

Figure 5. (a)(b) Two examples of template matching result, the red rectangles indicate the detected regions.

Extract the largest connected area *A* (with largest number of pixels) in the detected region obtained by template matching. We use the shape and location criteria based on the prior domain knowledge to determine whether it is CC.

$$A = \begin{cases} CC & if\ l_1/l_2 \geq T_S \quad and \quad l_d/l_h \leq T_L \\ other & otherwise \end{cases}. \quad (9)$$

Threshold T_S is set to 2 and T_L is set to 0.25 empirically to make sure that the CC structure is longer than the width, and located near the image center. Finally, the boundary of detected CC area is extracted as the initial contour of CC.

C. Geometric Active Contour (GAC) Based Segmentation

After the initialization of CC contour, the GAC model [7] is ready to capture the final segmentation of CC area.

Given an initial contour *C* of the CC area, representing the zero-level set of a signed distance function $\phi : \Re^2 \to \Re$, such that $\phi < 0$ inside the CC area, and $\phi > 0$ outside the CC area. The image gray scale intensities are modeled as the random variable $z \in Z$. Therefore, the probability density functions (PDFs) $p_{in}(z,\phi)$ and $p_{out}(z,\phi)$ of pixels inside and outside the contour *C* can be evaluated, respectively.

In the GAC model [7], the similarity between pixels inside and outside the contour *C* is measured by the standard deviation between the log-likelihood of $p_{in}(z,\phi)$ and $p_{out}(z,\phi)$. Therefore, the contour *C* is evolved iteratively to maximize the following image-based energy functional,

$$E(z,\phi) = \sqrt{\varepsilon\left[\left(\log\frac{p_{in}(z,\phi)}{p_{out}(z,\phi)}\right)^2\right] - \varepsilon\left[\left(\log\frac{p_{in}(z,\phi)}{p_{out}(z,\phi)}\right)\right]^2}, \quad (10)$$

where $\varepsilon[f(z)]$ denotes the expected value of the functional $f(z)$. The evolution of contour *C* (or equivalent ϕ) is performed according to the equation,

$$\frac{\partial\phi}{\partial t} = \nabla_\phi E(z,\phi). \quad (11)$$

The stopping criterion of evolution is that the maximum number of iterations is achieved.

III. Experimental Results

In this section, we present the performance of the proposed technique on 12 real brain MRI data. The ground truths of CC areas are manually drawn by a professional radiologist, and the segmentation results are compared with the ground truth data. To evaluate the segmentation performance, three evaluation metrics are computed as follows [11],

$$Accuracy = \frac{TP+TN}{TP+TN+FP+FN} \times 100\%, \quad (12)$$

$$Sensitivity = \frac{TP}{TP+FN} \times 100\%, \quad (13)$$

$$Specificity = \frac{TN}{TN+FP} \times 100\%. \quad (14)$$

where TP is the number of pixels in true positive area (region which is correctly classified as CC), TN is the number of pixels in true negative area (region which is correctly classified as background), FP is the number of pixels in false positive area (region which is incorrectly classified as CC), FN is the number of pixels in false negative area (region which is incorrectly classified as background).

In the experiment, we compare the segmentation performance between the MAC technique [12], the GAC technique [7], and the proposed technique. The MAC technique [12] is an active contour model based on image gradient information. The initial contours of CC in the MAC technique and the proposed technique are generated by the automated initialization technique described in section II. While for the GAC technique, a biggest possible rectangular is placed in the CC area for initialization, to approximate the automatically generated initial contour.

Fig. 6 presents examples of detection results based on the Magnetostatic Active Contour (MAC) technique [12] and the proposed technique. It is noticeable that the proposed technique has better performance in segmentation of CC. In addition, the comparison of statistical performance evaluation is shown in Table 1. It is observed that, the proposed technique outperforms the MAC technique [12] in all the indices. Because the proposed technique is based on the GAC framework, it achieves a similar segmentation performance with GAC technique [7].

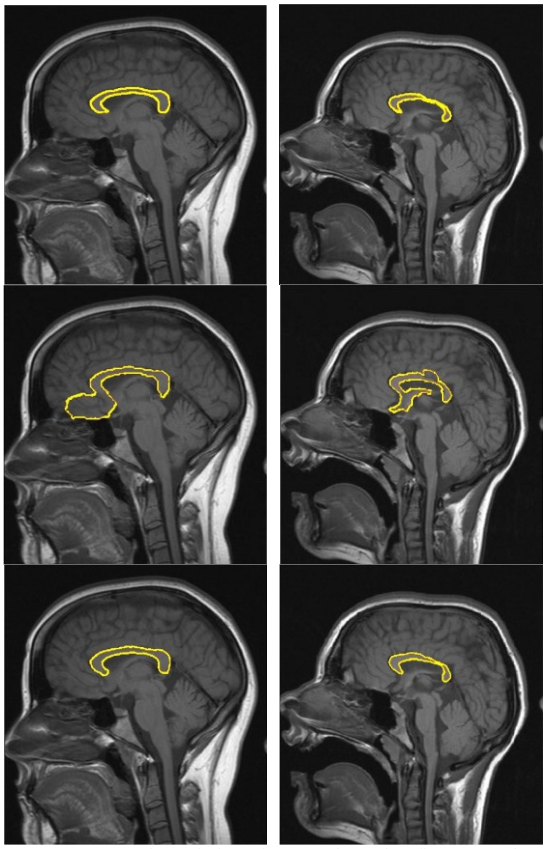

Figure 6. Two examples of detection results. The first row shows two T1-weighted midsagittal brain MRIs. The ground truths of CC structure are indicated by yellow contours. The second row and the third row (from top to bottom) illustrate the detection results based on the MAC technique [12] and the proposed technique, respectively. The detected CC structures are highlighted by yellow contours.

TABLE I. PERFORMANCE COMPARISON OF CC SEGMENTATION

Techniques	*Accuracy*	*Sensitivity*	*Specificity*
MAC [12]	85.67%	87.42%	89.70%
GAC[7]	91.35%	84.08%	93.30%
Proposed	**92.04%**	**86.88%**	**94.16%**

IV. CONCLUSION

This paper presents a simple and novel technique for the automated segmentation of CC in T1-weighted midsagittal brain MRIs. First, the initial brain MRI is clustered into various homogeneous areas using the adaptive mean shift technique. Second, the area analysis, template matching and the shape and location analysis are adopted to localize the CC area from generated clusters, and the boundary of obtained CC area is extracted as the initial contour of the subsequent deformation model. Finally, the segmentation of CC is generated using the Geometric Active Contour (GAC) model.

REFERENCES

[1] R. O'Dwyer, T. Wehner, E. LaPresto, L. Ping, J. Tkach, S. Noachtar, and B. Diehl, "Differences in corpus callosum volume and diffusivity between temporal and frontal lobe epilepsy", *Epilepsy & Behavior*, vol. 19, pp.376-382, 2010.

[2] A. Y. Hardan, N. J. Minshew, and M.S. Keshavan, "Corpus callosum size in autism", *Neurology*, vol. 55, no. 7, pp.1033-1036, Oct. 2000.

[3] J. Tong, Y. X. Sheng, W. Ying, and W. C. Dong, "A corpus callosum segmentation based on adaptive active contour model", in *Proc. 2nd Int. conf. Information Computing and Applications*, Beidaihe Qinhuangdao, 2011, pp.719-725.

[4] B. V. Ginneken, A. F. Frangi, J. J. Staal, B. M. T. H. Romeny, and M. A. Viergever, "Active shape model segmentation with optimal features", *IEEE Trans. Medical Imaging*, vol. 21, no.8, pp.924-933, Aug. 2002.

[5] A. El-Baz, A. Elnakib, M. F. Casanova, G. Gimel'Farb, A. E. Switala, and D. J. S. Rainey, "Accurate Automated Detection of Autism Related Corpus Callosum Abnonnalities", *The International Journal of Medical Systems*, vol. 35, no.5, pp.929-939, Oct. 2011.

[6] M. Jacob, T. Blu, and M. Unser, "Efficient Energies and Algorithms for Parametric Snakes", *IEEE Trans. Image Processing*, vol. 13, no.9, pp.1231-1244, Sep. 2004.

[7] R. Sandhu, T. Georgiou, and A. Tannenbaum, "A new distribution metric for image segmentation", in *Proc.* Society of PhotoOptical Instrumentation Engineers Medical Imaging 2008, vol.691404, 2008, pp. 1-9.

[8] A. Mayer and H. Greenspan, "An adaptive mean-shift framework for MRI brain segmentation", *IEEE Trans. Medical Imaging*, vol. 28, no.8, pp.1238-1250, Aug. 2009.

[9] T. Xu, I. Cheng, M. Mandal, "Automated Cavity Detection of Infectious Pulmonary Tuberculosis in Chest Radiographs", in *Proc.33rd Annu. Int. Conf. IEEE Engineering in Medicine and Biology Society*, Boston, 2011, pp.5178-5181.

[10] C. Lu, M. Mahmood, N. Jha, M. Mandal, "Automated Segmentation of the Melanocytes in Skin Histopathological Images", *IEEE Trans. Information Technology in Biomedicine*. In Press.

[11] T. Xu, M. Mandal, R. Long, I. Cheng, and A. Basu, "An edge-region force guided active shape approach for automatic lung field detection in chest radiographs", *Computerized Medical Imaging and Graphics*, vol. 36, no.6, pp.452-63, May, 2012.

[12] X. Xie and M. Mirmehdi, "MAC: Magnetostatic Active Contour Model", *IEEE Trans. Pattern Analysis and Machine Intelligence*, vol. 30, no. 4, pp. 632-646, Apr. 2008.